Buckling suppression of SiGe islands on compliant substrates

Haizhou Yin[a)]
Center for Photonics & Optoelectronic Materials and Department of Electrical Engineering,
Princeton University, Princeton, New Jersey 08544

R. Huang[b)]
Princeton Materials Institute and Department of Mechanical & Aerospace Engineering,
Princeton University, Princeton, New Jersey 08544

K. D. Hobart
Naval Research Laboratory, Washington, DC 20375

J. Liang and Z. Suo
Princeton Materials Institute and Department of Mechanical & Aerospace Engineering,
Princeton University, Princeton, New Jersey 08544

S. R. Shieh and T. S. Duffy
Department of Geoscience, Princeton University, Princeton, New Jersey 08544

F. J. Kub
Naval Research Laboratory, Washington, DC 20375

J. C. Sturm
Center for Photonics & Optoelectronic Materials and Department of Electrical Engineering,
Princeton University, Princeton, New Jersey 08544

A cap layer was used to suppress buckling during the relaxation of compressively strained 30 nm $Si_{0.7}Ge_{0.3}$ islands on borophosphorosilicate glass. The lateral expansion and buckling of a bilayer structure made of SiGe and a cap layer were studied by both modeling and experiment. Both epitaxial silicon and amorphous silicon dioxide (SiO_2) caps were investigated. Caps stiffen the islands to reduce buckling and accelerate the lateral relaxation, so that larger, flat, relaxed SiGe islands can be achieved. Using a 31 nm silicon cap, flat $Si_{0.7}Ge_{0.3}$ islands up to 200 μm$\times$200μm were achieved. However, germanium diffusion in the SiGe/Si structure took place during relaxation anneals and lowered the germanium fraction of the final fully relaxed SiGe film. Silicon dioxide caps, which are not prone to germanium diffusion, allowed suppression of SiGe buckling without lowering the germanium percentage. Full relaxation of SiGe islands was achieved by a controlled multicycle silicon dioxide removal and anneal procedure. Large, fully relaxed, smooth SiGe islands obtained using cap layers indicate that this approach could be of potential use for electronic device applications. © 2003 American Institute of Physics. [DOI: 10.1063/1.1621069]

I. INTRODUCTION

The goal of compliant substrates[1] is to allow strained heteroepitaxial semiconductors to relax to adjust the in-plane lattice constant. Compliant substrates usually include a means to decouple bulk substrate from epitaxial layers on top. Hobart *et al.*[2] used a viscous borophosphorosilicate (BPSG) compliant film to decouple the top epitaxial SiGe film from the underlying silicon substrate and demonstrated a method for creating relaxed SiGe films that in principle avoids the formation of dislocations. The work showed that the SiGe film remained flat on small islands, but buckled on large islands. In this article, we show that capping can be used to overcome the buckling problem.

Our previous work[3] investigated in detail the relaxation mechanism of SiGe islands on viscous BPSG films. The strain in SiGe islands relaxes by both lateral expansion and buckling (Fig. 1). Lateral expansion starts at the island boundary and then propagates toward the island center, so that larger islands expand much slower than smaller islands. In contrast, the rate of buckling does not depend on the island size. When a continuous SiGe film is patterned into small islands, these SiGe islands maintain a smooth surface during the relaxation as the strain relaxation is dominated by lateral expansion, which is much faster on smaller islands. In large SiGe islands where lateral expansion is slow, buckling of the SiGe film contributes to most of the relaxation and results in a rough surface, eventually leading to the fracture of the SiGe films when the surface roughness exceeds a critical value (Fig. 2). Although several methods were presented in our previous work to suppress buckling, the largest obtainable flat, relaxed SiGe island with a rms surface roughness less than 2 nm was only 60 μm wide, containing 30% germanium.

[a)]Electronic mail: hyin@ee.princeton.edu
[b)]Current address: Department of Aerospace Engineering and Engineering Mechanics, University of Texas, Austin, Texas 78712.
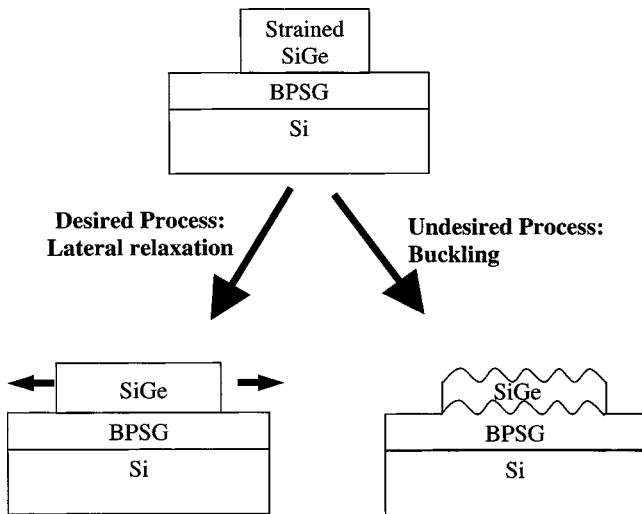
FIG. 1. Schematic of relaxation mechanisms: lateral expansion vs buckling. The SiGe film follows the BPSG profile.

This article presents a detailed study of buckling suppression using bilayer structures, made of a capping layer on the SiGe films. Both silicon and silicon dioxide are shown to be successful caps for alleviating buckling on large SiGe islands. Finally, limited instead of full relaxation in SiGe films, arising from the stress balance between the layers, is solved by the controlled removal of the capping layer.

II. EXPERIMENTAL PROCEDURE AND CHARACTERIZATION

Fully strained SiGe and strain-free Si films on BPSG are fabricated by wafer bonding and Smart-Cut® processes, which are the same as in Ref. 2 except that a 25 nm silicon cap was used for one sample. The donor wafer, which has the strained SiGe/unstrained Si films for transfer, was implanted with H_2^+ (180 KeV at dose of 4.5×10^{16} cm^{-2}). A silicon wafer coated with 200 nm BPSG (4.4% B and 4.1% P by weight) serves as the handle wafer. These wafers were
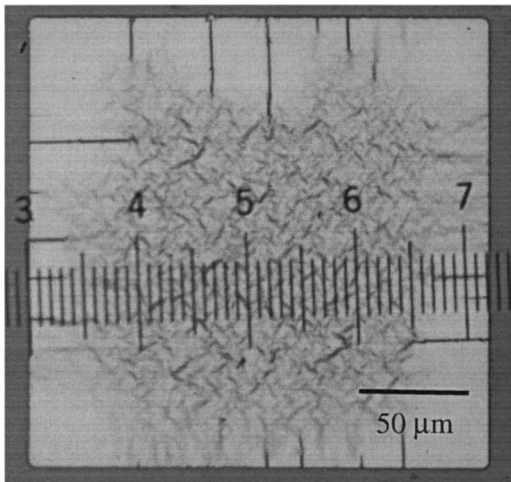

FIG. 2. Optical micrograph of a 200 μm×200 μm Si$_{0.7}$Ge$_{0.3}$ island on BPSG after a 5 h anneal at 800 °C in nitrogen. The rms surface roughness is larger than 15 nm. Many cracks formed during the annealing.

bonded at room temperature and then annealed at 250 °C for 4 h to strengthen the bonding, after which the wafer pair was annealed at 550 °C for 10 min to split the top substrate from the donor wafer at the depth of the hydrogen implantation. The residual silicon on the top was removed by selective etching. The resultant continuous SiGe/Si films were patterned into square islands of various sizes from 10 to 500 μm by reactive ion etch. In some cases, before annealing, capping layers of epitaxial silicon were grown on top of the SiGe layers at 700 °C by rapid thermal chemical vapor deposition (RTCVD), or amorphous SiO$_2$ layers were deposited by plasma enhanced chemical vapor deposition (PECVD) at 250 °C. At these temperatures, little relaxation of the structure is expected.

The strain in SiGe and Si films was locally measured by micro-Raman spectroscopy, using an Ar$^+$ laser (514.5 nm) focused to a spot of 3 μm. The Raman frequency shift associated with the Si–Si optical phonon mode in the SiGe and Si films was measured with an accuracy of ± 0.5 cm^{-1}. The strain ϵ_{Si} in the Si layer and the strain ϵ_{SiGe} in the Si$_{0.7}$Ge$_{0.3}$ layer were inferred from the Si–Si optical phonon frequency ω_{Si-Si} according to

$$\omega_{Si-Si}(Si) = 520 \text{ cm}^{-1} - 715\epsilon_{Si} \text{ cm}^{-1}, \text{[4]} \tag{1}$$

$$\omega_{Si-Si}(Si_{0.7}Ge_{0.3}) = 501 \text{ cm}^{-1} - 815\epsilon_{SiGe} \text{ cm}^{-1}. \text{[5]} \tag{2}$$

Atomic force microscopy was utilized to determine the surface roughness of SiGe films.

III. RESULTS AND DISCUSSION

A single compressive SiGe film on viscous glass relaxes by lateral expansion and buckling,[3] which have been modeled by Huang *et al.*[6] and Sridhar *et al.*,[7] respectively. The surface roughness depends on the relative rate of these two simultaneous processes, independent of the absolute time scale.[3,8] The surface roughens only when buckling occurs before the lateral expansion. Therefore, the key to improve surface roughness is to increase the ratio of the rate of lateral expansion over that of buckling, which is achievable by either speeding up lateral expansion or slowing down buckling. A bilayer structure, formed by a cap layer on the SiGe films, realizes both of the desired effects.

A. Accelerated lateral expansion in bilayer structures

As SiGe islands relax by lateral expansion, the strain at the center of the islands relaxes nearly exponentially over time.[6] The time scale for the relaxation is

$$\tau_L = \frac{\eta L^2}{c_{11SiGe} h_{SiGe} h_g}, \tag{3}$$

where L refers to the island edge length, η is the viscosity of the glass, h_g is the thickness of the glass, and c_{11SiGe} and h_{SiGe} are the elastic constant and the thickness of the SiGe film, respectively. In our experiments, h_g and h_{SiGe} are 200 and 30 nm, respectively. The time scale τ_L decreases as the thickness of the SiGe film increases. If one assumes a capping layer A on top of the SiGe, Eq. (3) can easily be modi-
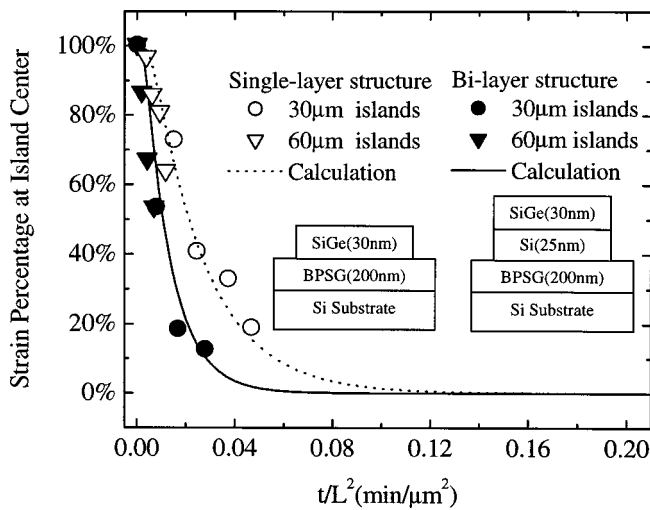
FIG. 3. Strain percentage at the SiGe island center, defined as 100% before relaxation and 0% upon equilibrium and measured by Raman spectroscopy, as a function of normalized annealing time at 800 °C for island size of 30 and 60 μm. Symbols are experimental data. The curved lines are from the lateral expansion model based on the parameters in Table I. The single-layer and bilayer islands are made of 30 nm $Si_{0.7}Ge_{0.3}$ and 30 nm $Si_{0.7}Ge_{0.3}$/25 nm Si, respectively.

fied if layers relax elastically. Following the same derivation detailed in Ref. 6, the time constant for lateral expansion of bilayer square islands on BPSG is

$$\tau_L = \frac{\eta L^2}{(c_{11SiGe}h_{SiGe} + c_{11A}h_A)h_g}, \tag{4}$$

where c_{11A} and h_A refer, respectively, to the elastic constant and the thickness of the film A, which forms a bilayer structure along with the SiGe film. Compared with the single-layer formula Eq. (3), it is clear that the bilayer can be treated as a single SiGe layer with an effective thickness

$$h_{SiGe}^{eff} = h_{SiGe} + \frac{c_{11A}}{c_{11SiGe}}h_A. \tag{5}$$

This increased effective SiGe thickness speeds up the lateral expansion of the islands, since the structure is now thicker and exerts more force on the compliant oxide.

For a single SiGe film, the lateral relaxation rate can be increased by increasing the SiGe thickness up to the critical thickness of the SiGe during its original growth, beyond which dislocations would form and render the film unacceptable for many applications. Adding a capping film to the SiGe layer increases the effective SiGe film thickness and circumvents the critical thickness constraint. In our experiments, the bilayer structure comprising 30 nm initially strained SiGe on top of 25 nm initially unstrained Si on 200

nm BPSG was fabricated using wafer-bonding and Smart-Cut® processes mentioned earlier in this article. Note that even though in this case the silicon layer is on the bottom, this does not affect the lateral expansion study of this bilayer structure. The strain at the center of islands ranging from 30 to 60 μm in edge width was measured as a function of annealing time at 800 °C in nitrogen (Fig. 3). Figure 3 also shows the strain relaxation of islands made of a single 30 nm SiGe layer on 200 nm BPSG, along with the theoretical calculations based on parameters listed in Table I. The viscosity η of the BPSG (1.1×10^{11} Poise at 800 °C) is extracted from lateral relaxation experiments in Ref. 3. It is clear that the bilayer islands reach equilibrium faster than their single-layer counterparts, confirming the accelerated lateral expansion in bilayer structures. The good agreement between experimental data and the calculation, as shown in Fig. 3, stresses the validity of the modified theory [Eq. (4)] for the bilayer structure. Finally, the data for the 30 and 60 μm islands in each case can be modeled via a single curve, showing that the relaxation time indeed scales as the square of the island edge width L.

B. Suppressed buckling in bilayer structures

In addition to having a faster lateral expansion rate, the bilayer structure has a much slower buckling growth rate than a single-layer structure. Sridha *et al.*[7] have proposed a theory for single-layer buckling on compliant BPSG, which describes the surface buckling as a superposition of many exponentially growing modes. Each mode is a sinusoidal surface profile, whose amplitude rises exponentially over time:[7]

$$A(t) = A_0 e^{t/\tau_B}, \tag{6}$$

where A is the surface roughness, A_0 is the initial surface roughness, and τ_B is the buckling time constant, which is determined by[7]

$$\frac{1}{\tau_B} = \frac{1}{2\eta}\left[\frac{\sinh(2h_gk) - 2h_gk}{1 + \cosh(2h_gk) + 2(h_gk)^2}\right]\left[\frac{E_{SiGe}\epsilon_{SiGe}h_{SiGe}k}{1-\nu}\right. \\ \left. - \frac{E_{SiGe}h_{SiGe}^3}{12(1-\nu^2)}k^3\right], \tag{7}$$

where E_{SiGe} and ν are the Young's modulus and Poisson's ratio of the SiGe film, respectively, and k is the wave number of the mode. In the case where a capping film A is on the SiGe layer, following the derivation in Ref. 7 for layers without caps, one can derive the new equation for the buckling growth rate:

TABLE I. Mechanical properties of $Si_{0.7}Ge_{0.3}$ (linearly interpolated between Si and Ge), Si, and SiO_2 at 800 °C for lateral expansion and buckling calculations in this study.[a]

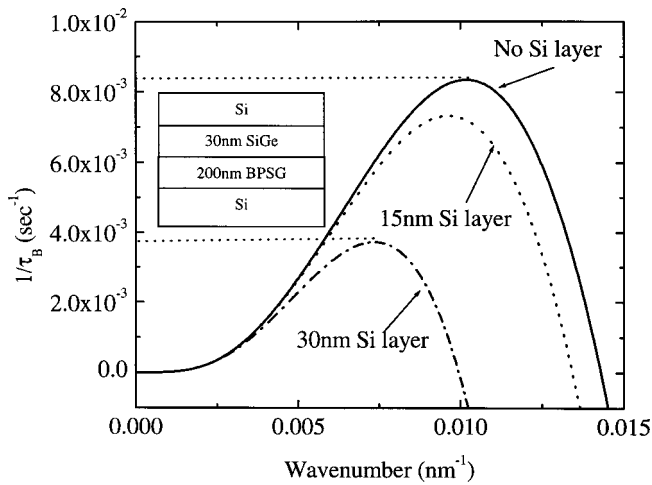| $E(Si_{0.7}Ge_{0.3})$ (10^{10} N/m²)	$c_{11}(Si_{0.7}Ge_{0.3})$ (10^{10} N/m²)	$E(Si)$ (10^{10} N/m²)	$c_{11}(Si)$ (10^{10} N/m²)	$E(SiO_2)$ (10^{10} N/m²)	ν
11.3	14.3	12.1	15.4	6.1	0.28

[a]See Refs. 3 and 9–12.

FIG. 4. Calculated buckling growth rate ($1/\tau_B$) as a function of buckling wave number, based on Eq. (8) and parameters in Table I. This calculation assumes an infinite film in which lateral expansion is absent.

FIG. 5. Surface roughness vs annealing time in nitrogen for silicon caps of thickness 0, 19, and 31 nm, measured at the center of 200 μm$\times$200 μm Si$_{0.70}$Ge$_{0.30}$ islands.

$$\frac{1}{\tau_B} = \frac{1}{2\eta}\left[\frac{\sinh(2h_g k) - 2h_g k}{1 + \cosh(2h_g k) + 2(h_g k)^2}\right]$$

$$\times \left[\frac{(E_{SiGe}\epsilon_{SiGe}h_{SiGe} + E_A \epsilon_A h_A)k}{1-\nu}\right.$$

$$\left. - \frac{(E_{SiGe}h_{SiGe}^3 + E_A h_A^3)}{12(1-\nu^2)}k^3\right]. \qquad (8)$$

E_A and ϵ_A represent the Young's modulus and strain of the film A, respectively. Its Possion's ratio is assumed to be the same as the SiGe film for simplicity, which is a good approximation for Si and SiO$_2$ used in this study. Note that with the absence of film A (i.e., h_A is zero), Eq. (8) is exactly reduced to Eq. (7). To illustrate the effect of the capping film A on the buckling, the buckling growth rate versus the buckling wave number is plotted in Fig. 4 based on Eq. (8), using Si as the capping layer. The initial strain in the capping silicon layer is set to be zero because the SiGe film still has the in-plane lattice constant of its original Si substrate. Note that the dominant buckling occurs at the wavelength where the buckling growth rate is highest. The addition of a 30 nm silicon layer can lower the maximum buckling growth rate by a factor of two, from 8.2×10^{-3} to 3.8×10^{-3} s^{-1} (Fig. 4). Two physical effects cause the reduction in the buckling growth rate: (i) the bilayer structure is more mechanically rigid and thus less likely to bend, and (ii) the buckling driving force, the average strain, is now less with a cap than without a cap because the added film is initially strain free.

This predicted buckling suppression by a silicon layer was verified in experiments. Epitaxial Si films of several thicknesses were deposited on fully compressive 30 nm Si$_{0.7}$Ge$_{0.3}$/200 nm BPSG using RTCVD at 700 °C. The Si/SiGe bilayers were then annealed and the time dependence of the surface roughness at the center of 200 μm$\times$200 μm islands was measured for different cap thicknesses (Fig. 5). Because negligible lateral expansion occurred at the center of 200 μm islands during the anneal, the buckling behav-
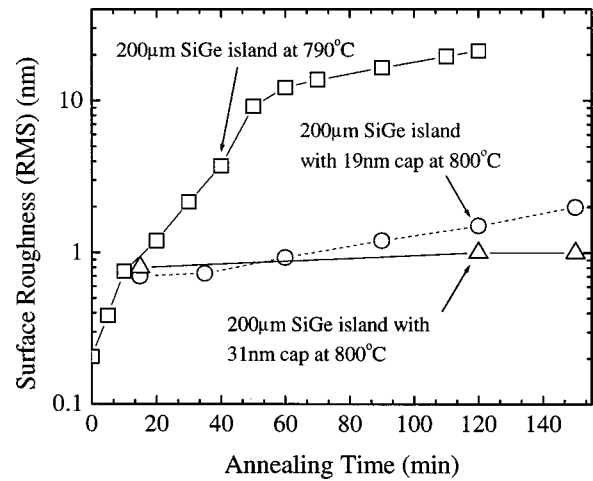
ior of the islands is the same as that of infinite films. A 19 nm silicon cap can reduce buckling after a 2 h anneal from 20 nm to less than 2 nm, and with a 31 nm cap, the buckling is decreased to 1 nm.

C. Large, flat, and fully relaxed SiGe islands

1. Epitaxial silicon cap layers

A capping layer speeds up lateral expansion while the buckling growth rate is suppressed. Therefore, much larger flat islands should be achievable than with a single SiGe film alone. The first experiment utilized a 19 nm silicon cap layer deposited by RTCVD on patterned 30 nm SiGe, as mentioned in the previous section. The surface roughness at the center of islands was measured versus annealing time for islands of edge widths 100, 200, and 500 μm. Figure 6(a) shows that the 100 μm island remained flat (rms$\sim$1 nm) throughout the entire anneal. This is far larger than the largest flat island of 60 μm achieved using a single 30 nm SiGe film without a cap.[3] The 200 μm island initially buckled to an rms roughness of $\sim$5 nm after 300-min annealing at 800 °C, and then flattened out (rms$<$2 nm) when the lateral expansion finally reached the center after long annealing (22 h at 800 °C and 6.5 h at 850 °C) [Fig. 6(b)]. The 500 μm island still buckled dramatically (rms$>$10 nm), and many cracks resulted from the local strain in the buckled regions [Fig. 6(c)]. To achieve larger flat islands, a thicker Si cap layer ($\sim$31 nm) was then tested. Figure 7(a) shows the surface roughness at the center of 200 and 500 μm islands as a function of annealing time. The buckling on the 200 μm island previously observed in Fig. 6(a) disappeared, and the roughness was less than 2 nm. Although the roughness grew on the 500 μm island, it was much slower than with a 19 nm silicon cap, and in this case, only one crack is seen on the 500 μm island [Fig. 7(b)].

Although the Si cap considerably increases the size of obtainable flat SiGe islands, the SiGe islands are not fully relaxed upon equilibrium. The final strain in the SiGe film is governed by the stress balance between the films and can be shown to be.[9]
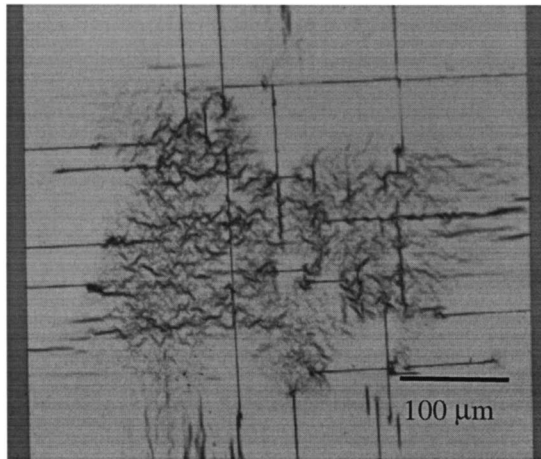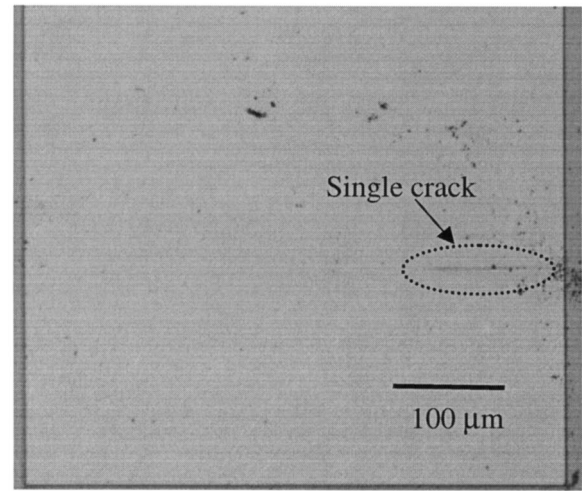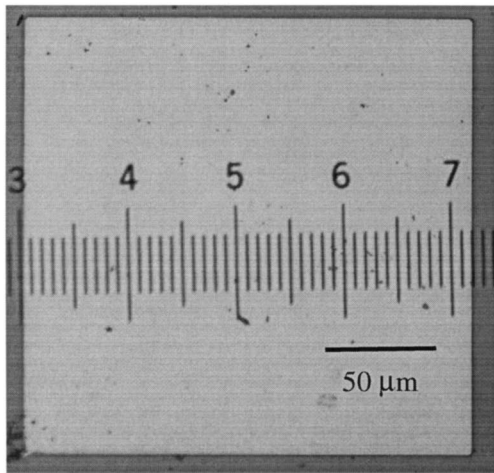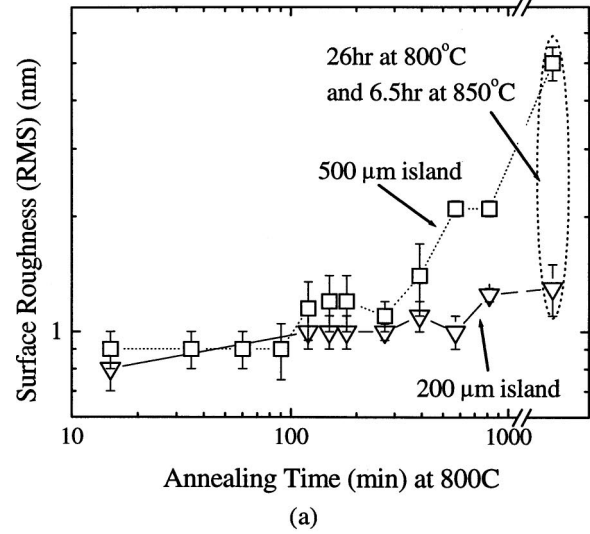
(a)

(b)

(c)

FIG. 6. (a) Surface roughness vs annealing time in nitrogen at 800 °C for a 19 nm silicon cap, measured at the center of islands of size 100, 200, and 500 μm. The points after the break on the time axis represent 22 h annealing at 800 °C, followed by another 6.5 h anneal at 850 °C. (b) Optical micrograph of a 200 μm×200 μm island after annealing. Rms surface roughness at the island center is about 1.6 nm. (c) Optical micrograph of a 500 μm ×500 μm island after annealing. Rms surface roughness at the island center is larger than 10 nm.
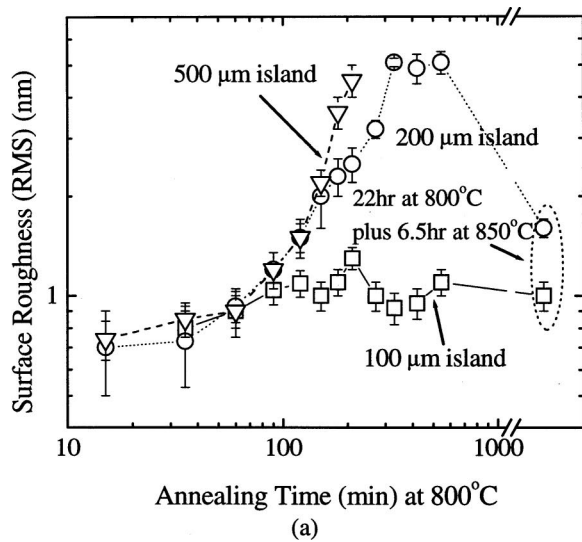

(a)

(b)

FIG. 7. (a) Surface roughness vs annealing time at 800 °C for a 31 nm Si cap, measured at the center of islands of 200 and 500 μm in edge width. (b) Optical micrograph of a 500 μm×500 μm island after a 26 h anneal at 800 °C, followed by a 6.5 h anneal at 850 °C. Rms surface roughness at the island center is about 5 nm.

$$\epsilon_{\text{SiGe\_final}} = \epsilon_{\text{SiGe\_initial}} \frac{E_{\text{Si}} h_{\text{Si}}}{E_{\text{SiGe}} h_{\text{SiGe}} + E_{\text{Si}} h_{\text{Si}}}, \qquad (9)$$

where $\epsilon_{\text{SiGe\_initial}}$ is the initial strain in the SiGe film and Poisson's ratio is assumed the same in Si and SiGe films. Figure 8 shows the final strain in the SiGe films on islands up to 80 μm in edge width upon equilibrium (annealed for 3 h at 800 °C). Germanium diffusion during this relaxation anneal is negligible as the annealing time needed for small islands to reach stress balance is relatively short. From an initial strain of 1.2%, a final strain 0.43% in the SiGe film with a 19 nm silicon cap is observed, independent of the island size, which agrees well with the prediction of Eq. (9) of 0.47%. Increasing the cap thickness to 31 nm increases the final strain in the SiGe film to 0.61%, which also shows a good agreement between the experimental data and the stress balance theory. A thicker silicon cap clearly results in more final strain in the SiGe film at stress balance.
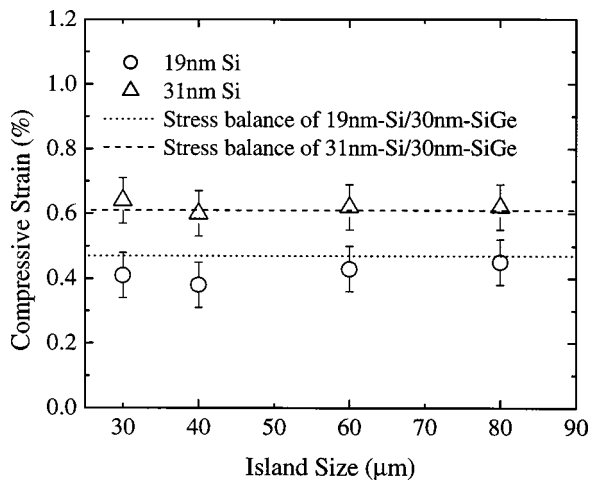
FIG. 8. Biaxial strain of 30 nm $Si_{0.70}Ge_{0.30}$ and Si at island center as a function of island sizes after a 3 h anneal at 800 °C. Open symbols are experimental data. Lines are calculation of stress balance based on the parameters in Table I. All Si/SiGe islands have reached equilibrium and the silicon cap clearly prevents full relaxation of the strain in SiGe films.

FIG. 9. Raman spectra measured at the center of a 30 μm×30 μm island comprising 31 nm Si/30 nm $Si_{0.7}Ge_{0.3}$. The dashed line reflects the stress balance between the Si and $Si_{0.7}Ge_{0.3}$ films after a short anneal (210 min at 800 °C). The solid line indicates that the Si and $Si_{0.7}Ge_{0.3}$ films have intermixed after a long anneal (13 h at 850 °C). The peak at 520 cm^{-1} comes from the silicon substrate.

To realize full relaxation in the SiGe film, the silicon layer should be removed after the initial anneal and a further anneal should be performed. In this second anneal, buckling is less likely to be a problem, even without the cap, because the strain in the SiGe film is less than that before the first anneal and the buckling growth rate depends on the strain in the SiGe film [Eq. (8)]. The removal of the Si cap is feasible only if little germanium diffusion occurs during the relaxation annealing. Otherwise, the Si and SiGe films can intermix and form a single SiGe layer with a smaller germanium percentage. Given the long annealing required to reach equilibrium on large islands, considerable germanium diffusion does take place between the Si and SiGe films. This was confirmed by Raman spectroscopy for a 30 nm $Si_{0.7}Ge_{0.3}$ layer with a 31 nm silicon cap. Before long annealing, two distinct Si–Si phonon peaks (516 cm^{-1} for the Si layer and 507 cm^{-1} for the $Si_{0.7}Ge_{0.3}$ layer) were visible (Fig. 9). After a 13 h annealing at 850 °C a single Si–Si phonon peak was observed at 510.5 cm^{-1}. This corresponds to a relaxed $Si_{0.85}Ge_{0.15}$ layer, which would be expected from mixing 31 nm Si and 30 nm $Si_{0.7}Ge_{0.3}$ films. (The Raman peak at 520 cm^{-1} comes from the silicon substrate and relaxed $Si_{0.7}Ge_{0.3}$ would have a Raman peak at 501 cm^{-1}) This single SiGe film is undesirable because its in-plane lattice constant is not as large as the fully relaxed SiGe film with the original germanium percentage. To avoid germanium diffusion during the relaxation annealing, a different material is needed for the cap layer.

2. Silicon dioxide capping layers

The suppression of buckling depends solely on the mechanical property of the cap layer. Therefore, any rigid film that will not crack or flow can be used as the cap to suppress buckling. Since germanium diffusion in silicon dioxide is very slow, silicon dioxide is a good candidate for the cap material. A layer of 130 nm SiO_2 was deposited on 30 nm $Si_{0.7}Ge_{0.3}$ by PECVD at 250 °C to form an alternate

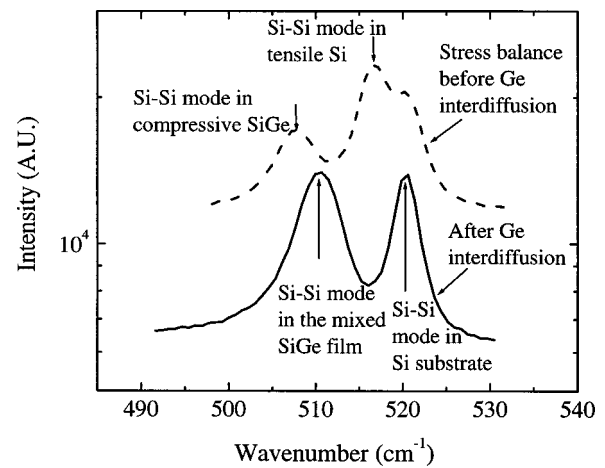bilayer structure, which was then patterned into islands of edge widths from 30 to 200 μm. After a 3 h anneal at 875 °C, the $Si_{0.7}Ge_{0.3}$ and SiO_2 films in islands up to 100 μm wide reached stress balance. The compressive strain in the SiGe film, measured by Raman spectroscopy, decreased from 1.2% to 0.8%, which is consistent with the stress balance theory. In addition, all islands remained smooth (rms<1 nm) after this anneal.

To further relax the strain, the oxide cap needs to be removed. The residual strain in the SiGe film can still lead to buckling if the oxide cap is removed entirely at once. In the extreme case when all oxide was removed after the initial stress balance, it was found that during the subsequent annealing, the 0.8% strain in the SiGe film caused dramatic buckling on islands as small as 60 μm wide. Therefore, a multicycle process was performed in which the cap was thinned and then annealed again to reach stress balance in each cycle. After the initial relaxation process to achieve stress balance, about one-seventh (19 nm) of the SiO_2 cap was removed using dilute hydrofluoric acid. This thinned SiO_2/SiGe sample was annealed again to reach a new stress balance, at which the SiGe film was less compressive and thus less likely to buckle. This etch-and-anneal process was repeated seven times to remove the entire cap and to allow the SiGe layer to fully relax without buckling. The strain in the SiGe film measured by Raman spectroscopy at the island center after each cycle is plotted for islands of size 30, 100, and 200 μm [Fig. 10(a)]. Also shown is the calculated strain after each cycle based on the oxide thickness and assuming stress balance was reached after each anneal. The final surface roughness for islands of various sizes after the cap removal and anneals is shown in Fig. 10(b). The islands of up to 100 μm in edge width remained flat (rms~1 nm) and reached full relaxation after the oxide cap was removed completely, whereas the 200 μm island was quite rough (rms~8 nm) and retained some residual strain. Note that the strain in the 200 μm island is generally above the strain predicted by
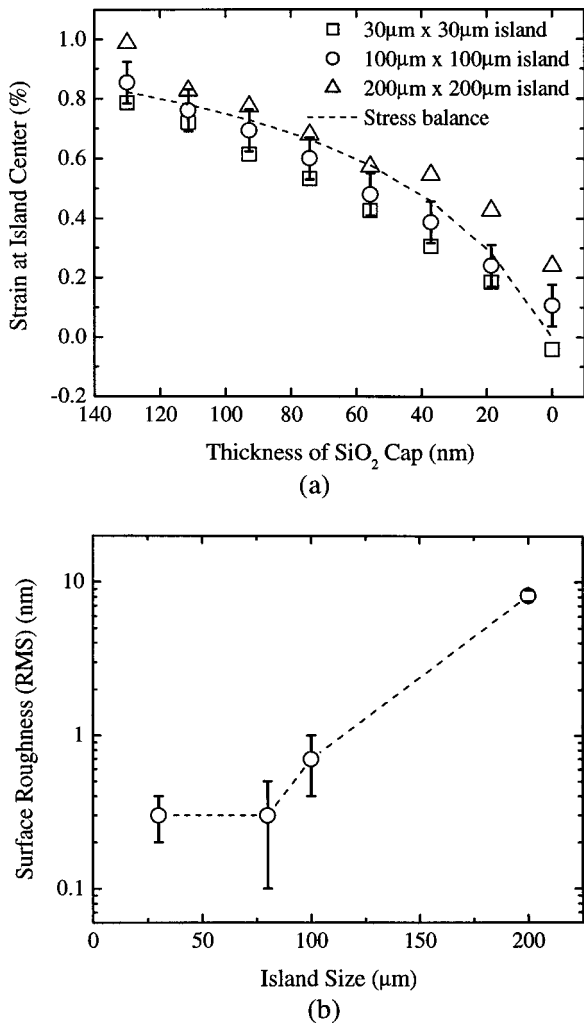
(a)

(b)

FIG. 10. (a) Progression of biaxial strain in the $Si_{0.7}Ge_{0.3}$ film after an initial 3 h anneal at 875 °C and seven cap-thinning cycles with an anneal at 875 °C for 3 h for each. The open symbols represent the measured strain at the center of islands of 30, 100, and 200 μm in edge width. The dashed line is a prediction by stress balance theory using the oxide thickness of each step. (b) Rms surface roughness of islands as a function of island size after seven cap-thinning cycles. Islands up to 100 μm remain flat.

the stress balance during the thinning process, indicating that stress balance has not been reached in the large islands after annealing. The rough surface on the 200 μm island arose from the last thinning step, in which the strain (0.25%) was still large and all of the oxide cap, which suppresses buckling, was removed.

To potentially reduce the final roughness and reduce the number of etch-and-anneal cycles, we theoretically analyzed the thinning process. Two different thinning strategies were considered: an "equal-step" thinning process and an "unequal-step" thinning process. For both processes, the structure is first annealed to stress balance before the cap is thinned. For the equal-step process, as in the above experiment, the SiO_2 cap is thinned by an equal amount in each cycle, with each followed by an anneal. For the unequal-step process, the oxide cap is thinned by half of its remaining thickness in each cycle (except for the last one when all residual oxide is removed), with each etch step followed by an anneal. For each cycle in the thinning process, one can
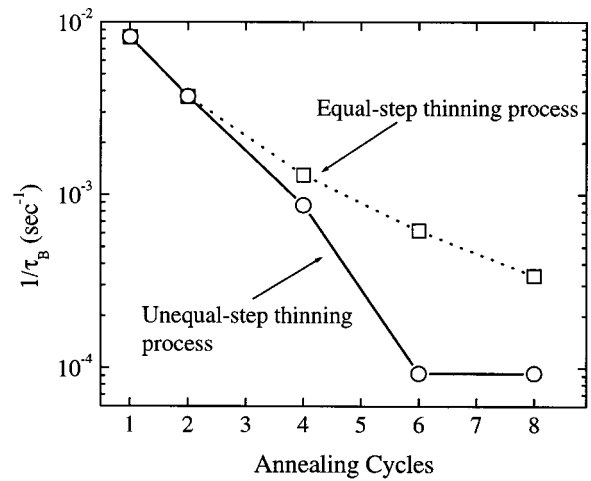

FIG. 11. The maximum buckling growth rate as a function of the annealing cycles for a 130 nm SiO_2 cap on 30 nm $Si_{0.7}Ge_{0.3}$, calculated from Eq. (8) based on parameters in Table I. The open squares represent the equal-step thinning process, in which same amount of the oxide cap is etched for each step. The open circles represent the unequal-step thinning process, in which the oxide cap is thinned down 50% in each cycle. Note that for the final cycle, the cap is completely removed before annealing, which is equivalent to the no-cap case [Eq. (7)].

calculate the maximum buckling growth rate $1/\tau_B$. Note the wavelength at which the largest $1/\tau_B$ occurs will vary as the strain and thickness change (as was seen in Fig. 4). The final roughness is assumed to be dominated by the buckling with the largest $1/\tau_B$. Therefore, effectiveness of buckling suppression in different thinning processes can be compared, to first order, using the highest buckling growth rate of all cycles. This is shown in Fig. 11 as a function of the number of annealing cycles for both equal-step and unequal-step processes. Because the strain relaxed in each etch-and-anneal cycle decreases as the number of annealing cycles increases, a thinning process with more annealing cycles is less prone to buckling. The superior buckling suppression by the unequal-step thinning process over the equal-step thinning process as shown in Fig. 11 stems from a better-controlled balance between relieved strain in each cycle and the thickness of the remaining oxide cap. Using the unequal-step thinning process, more strain is relaxed when the oxide cap is thicker. This translates to less strain relaxation when the oxide cap is thin, when the structure is most prone to buckling. However, the highest buckling growth rate in the unequal-step thinning process does not always decrease as more annealing cycles are added. In the unequal-step thinning scheme, only when the highest buckling growth rate occurs at the last cycle can be addition of annealing cycles further decrease the highest buckling growth rate. This explains why the highest buckling growth rate remains unchanged when the number of annealing cycles increases from six to eight, as the highest buckling growth rate for the eight-cycle process takes place in the fourth cycle. To further optimize the thinning process so as to minimize annealing cycles while maintaining a small buckling growth rate, one should consider the competition between buckling and lateral expansion at each step and devise a more efficient thinning scheme,
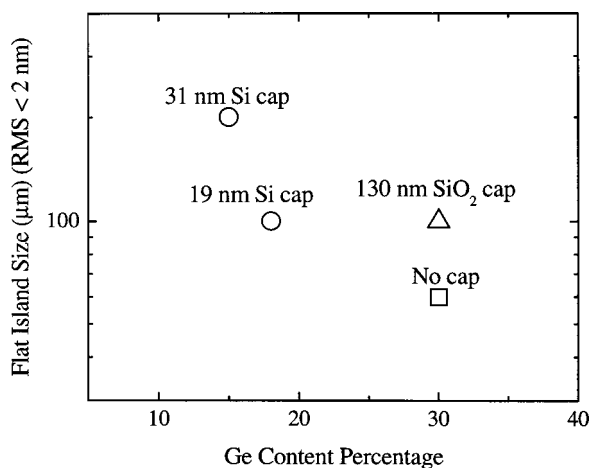
FIG. 12. Summary of the size and germanium percentage of flat, relaxed, SiGe islands obtained using various cap techniques. Capping layers, made of either Si or SiO$_2$, dramatically increase the size of achievable flat islands.

which could combine the equal-step, unequal-step, or other thinning processes.

Both the germanium percentage and the size of the achievable flat, relaxed, SiGe islands are critical for relaxed-SiGe based applications. With the use of capping layers to suppress buckling and cap removal to allow full relaxation, we have been able to obtain large, flat islands with 30% germanium. Figure 12 summarizes our results obtained through various cap techniques. Without any capping film, the size of largest, flat, relaxed Si$_{0.7}$Ge$_{0.3}$ islands is limited to 60 μm, beyond which islands buckle and crack during relaxation. Using a 31 nm silicon cap, flat islands as large as 200 μm have been made but the germanium percentage is lowered ($\sim$15%) as a result of germanium diffusion in Si/SiGe layers. The adoption of oxide as the capping material circumvents the germanium diffusion problem and enables cap removal after stress balance, increasing flat island size (100 μm islands for 130 nm SiO$_2$) for 30% germanium layers.

IV. SUMMARY

Both silicon and silicon dioxide capping layers were successfully utilized to suppress the buckling of large, compressively strained SiGe islands during their relaxation on BPSG. Theories for lateral expansion and buckling of bilayer structures on BPSG were developed. The lateral expansion was accelerated and the buckling was impeded by the added cap layer. Although the silicon cap is effective in buckling suppression, germanium diffusion during relaxation anneals made full relaxation of the SiGe islands difficult. The use of silicon dioxide caps avoided this problem, and a multicycle SiO$_2$ thinning process enabled fully relaxed Si$_{0.7}$Ge$_{0.3}$ islands on BPSG to be achieved. The large, flat, and strain-free Si$_{0.7}$Ge$_{0.3}$ islands that have been obtained are a promising platform for electronic devices.

ACKNOWLEDGMENT

[1] Y. H. Lo, Appl. Phys. Lett. **59**, 2311 (1991).
[2] K. D. Hobart, F. J. Kub, M. Fatemi, M. E. Twigg, P. E. Thompson, T. S. Kuan, and C. K. Inoki, J. Electron. Mater. **29**, 897 (2000).
[3] H. Yin, R. Huang, K. D. Hobart, Z. Suo, T. S. Kuan, C. K. Inoki, S. R. Shieh, T. S. Duffy, F. J. Kub, and J. C. Sturm, J. Appl. Phys. **91**, 9716 (2002).
[4] D. J. Lockwood and J.-M. Baribeau, Phys. Rev. B **45**, 8565 (1992).
[5] J. C. Tsang, P. M. Mooney, F. Dacol, and J. O. Chu, J. Appl. Phys. **75**, 8098 (1994).
[6] R. Huang, H. Yin, J. Liang, K. D. Hobart, J. C. Sturm, and Z. Suo, Mater. Res. Soc. Symp. Proc. **695**, 115 (2001).
[7] N. Sridhar, D. J. Srolovitz, and Z. Suo, Appl. Phys. Lett. **78**, 2482 (2001).
[8] J. Liang, R. Huang, H. Yin, J. C. Sturm, K. D. Hobart, and Z. Suo, Acta Mater. **50**, 2933 (2002).
[9] H. Yin, K. D. Hobart, S. R. Shieh, T. S. Duffy, F. J. Kub, and J. C. Sturm, Appl. Phys. Lett. **82**, 3853 (2003).
[10] M. Newberger, *Group IV Semiconducting Materials*, Handbook of Electronic Materials Vol. 5 (IFI/Plenum, New York, 1971).
[11] S. P. Nikanorov, Yu. A. Burenkov, and A. V. Stepanov, Sov. Phys. Solid State **13**, 2516 (1971).
[12] S. P. Nikanorov and B. K. Kardashev, *Elasticity and Dislocation Inelasticity of Crystals* (Nauka, Moscow, 1985) [in Russian].